Archives of Civil and Mechanical Engineering (2025) 25:28
https://doi.org/10.1007/s43452-024-01088-0

ORIGINAL ARTICLE

Fuzzy logic as a method of analysis of hot forging process of 80MnSi8-6 steel

Marek Wojtaszek[1] · Grzegorz Korpała[2] · Krystian Zyguła[1] · Kamil Cichocki[1] · Karolina Kowalczyk[3] · Wiktoria Skonieczna[1] · Barbara Mrzygłód[1] · Ulrich Prahl[2] · Magdalena Barbara Jabłońska[4]

Received: 29 August 2024 / Revised: 25 October 2024 / Accepted: 1 November 2024

Abstract

A novel approach was proposed, based on the application of the fuzzy logic (FL) method for the fast analysis of the hot deformation process of 80MnSi8-6 steel. In the first stage, the curves developed from plastometric tests and the results of studies of the microstructure of the deformed samples were used as input data for the analysis. Input and output variables were adopted and a set of rules based on cause-and-effect relationships was defined, defining the interactions between the variables. A fast FL-controller was designed, and the correctness of its operation was verified by comparison with experimental results and the results of finite element method (FEM) analysis, carried out taking into account the evolution of the microstructure. The process of hot compression under isothermal conditions of 80MnSi8-6 steel specimens was simulated on the Warmumformsimulator (WUMSI), assuming such parameters and other conditions as were used in real tests. It was confirmed that the proposed method, based on the analysis of flow curves and prior austenite grain size using a fuzzy controller, gave satisfactory results. Subsequently, a novel FL-controller was developed to analyze the kinetics of dynamic recrystallization (DRX), using data obtained from the author's model of this phenomenon for its construction and calibration. The correctness of the controller was confirmed by comparing the results of its DRX volume fraction calculations with the distributions of this value determined by the model and the model-based FEM analysis method, respectively. It was shown that FL is applicable also when a model of the analyzed phenomenon is available. Unlike model-based calculations, a properly designed controller allows the indication of deviations from general trends that can be pointed out and interpreted by a human expert, but significantly faster. It can also serve as a component of a system analyzing complex processes, such as hot multi-stage forging. Fuzzy controller can be used in parallel with modeling or replace models in calculations.

Keywords Hot metal forming · Fuzzy logic · FL-controller · Microstructure evolution · 80MnSi8-6 steel

1 Introduction

Structural steels are currently among the most widely used materials in engineering. They are produced through well-understood and technically mastered processes and are characterized by high and stable properties [1]. Within this group of materials, bainitic steels are gaining increasing significance. Bainite is a phase aggregate composed of ferrite plates with minor phases such as retained austenite and carbides [2]. Bainitic microstructures can be generated throughout the entire volume of products or in selected areas [3], such as the near-surface region. The mechanical properties of bainitic steels are high and competitive compared to many conventional steels [4]. The size of the bainitic constituents can be controlled within a range from tens of nanometers to hundreds of micrometers [5]. By controlling

✉ Marek Wojtaszek
wojtaszek@agh.edu.pl

1 Faculty of Metals Engineering and Industrial Computer Science, AGH University of Krakow, Al. Mickiewicza 30, 30-059 Kraków, Poland

2 Institut für Metallformung, TU Bergakademie Freiberg, 4 Bernhard-von-Cotta-Straße, 09599 Freiberg, Germany

3 Institute of Materials Engineering, University of Silesia, 75 Pułku Piechoty 1a, 41-500 Chorzów, Poland

4 Łukasiewicz Research Network - Institute of Non-Ferrous Metals in Gliwice, Sowińskiego 5, 44-101 Gliwice, Poland

Published online: 14 November 2024

the microstructural scale, the properties of the products can be significantly modified [6], depending on their intended use. A typical bainitic ferrite plate has a thickness of about 0.2–0.5 µm and an average length of about 100 µm [7]. By controlling plastic deformation and heat-treatment processes, microstructures typical of nanobainitic steels can be achieved, consisting of a mixture of very thin bainitic ferrite plates separated by carbon-enriched austenite [8]. Steel manufacturers and users of these products have recognized the advantages of obtaining this type of microstructure [9]. One of the most important advantages of nanobainitic steels is the highly favorable combination of strength and ductility, compared to many high-performance steels [10]. Nanostructured bainitic steel induced by quasi-static and dynamic deformation can achieve a mostly higher combination of hardness and strength with no brittle cracking at even very high strain rates [11]. The presence of nanobainite also results in high wear resistance [12], as demonstrated in studies conducted by Leiro et al. [13] and Du et al. [14]. The ability to modify the properties of nanobainitic steel also opens up possibilities for producing products with special requirements, such as protective armor [15]. Due to the high application potential of nanobainitic steels, they are currently the subject of intensive research. It is generally accepted that they must be cost-effective to produce, which can be achieved by excluding expensive elements such as cobalt and nickel from the chemical composition. Bainite subunits thinner than 100 nm are most commonly obtained by performing isothermal heat treatment in the temperature range of 200–400 °C [4]. In many studies focused on designing nanobainitic steels, the primary goal is to achieve nanobainite at the lowest possible temperature [8]. Research conducted by Garcia-Mateo et al. [16] has considered the economic benefits achieved using inexpensive alloying elements and enabling transformation within an industrially acceptable time frame.

The favorable combination of strength, ductility, and performance properties of nanobainitic steels makes these materials potentially suitable for producing medium- and large-sized structural components. These components are typically shaped through open-die forging operations, and then air-cooled. However, the heat treatment time required to achieve a uniform bainitic microstructure in large forgings can be measured in days, leading to excessive usage of heating installations [17] and making the process costly. On the other hand, nanobainitic steels can be used for the open-die forging of small series of structural components with significantly smaller dimensions, such as shafts, rings, and bushings. A limitation of open-die forging technology is the need for multiple operations, which requires a long processing time. This time depends primarily on the strain value and the shape of the component. As a result, inter-stage reheating is often necessary, which is costly, energy-intensive, and leads to grain growth (GG). This issue is particularly relevant for forgings weighing up to several dozen kilograms, which quickly lose heat to the environment and tools [18]. Therefore, when using this hot-forming method for bainitic steels, it is crucial to design the successive operations in such a way that minimizes the need for inter-stage reheating while also achieving a microstructure with the finest possible prior austenite grain size, which is most favorable for transformation into nanobainite in the subsequent step. This approach was the focus of the work [18], which demonstrated that an integrated modeling method is useful for designing the forming processes of the studied bainitic steel when multiple consecutive operations are involved.

Due to the large number of operations and the rapid cooling of the material, optimizing the design of the multi-stage forging process for small forgings is complex. Additional challenges include accounting for the specific characteristics of a given production line, such as factors affecting the rate of heat loss from the material during successive forging operations and the necessary pauses between them. Therefore, in the implementation of multi-stage hot forging technology for many modern materials, including bainitic steels, the role of the human expert is crucial. However, the limitation in such cases is the relatively long time required for analysis and response. One method to address this problem is the use of a computational tool that enables the analysis of the problem in a way that corresponds to the actions of a human expert but completes the task in significantly less time. An example of such a tool are expert systems. However, their application requires deep knowledge of the material being shaped and the process, particularly the development of quantitative and qualitative cause-and-effect relationships between the hot deformation parameters and the material's behavior during the process, as well as the evolution of its microstructure [19]. Currently, these relationships are determined based on data from plastometric tests and metallographic studies of deformed samples [20].

In cases where hot forging processes are designed, predominantly involving compressive stresses, material response to the applied deformation parameters is commonly described using hot compression tests under constant temperature and strain rate conditions. These tests are conducted within parameter ranges relevant to the material under investigation and possibly achievable with the available production line. Developing and analyzing flow curves allows for the identification of key phenomena associated with hot deformation, such as work hardening (WH), dynamic recovery (DRV), and dynamic recrystallization (DRX). It also facilitates the analysis of interactions among these phenomena. These data are combined with observations and assessments of the microstructure of deformed samples. Analysis of this information by an human expert enables the identification of parameter combinations that result in favorable microstructures and, consequently, the desired product properties. It also helps in selecting parameter ranges to avoid, as they may lead to the formation of micro or macrostructural defects. Research in this area has also been conducted by the authors of this publication, with selected results presented in [18, 21]. However, the analysis and interpretation of data by experts is time-consuming. This issue can be eliminated using solutions based on expert systems, including controllers that perform calculations using fuzzy logic (FL).

In the simplest terms, expert systems are programs designed to process and autonomously interpret human expert knowledge. They are typically developed to address issues for which creating a high-quality mathematical model is either impossible or economically unfeasible. A key characteristic of expert systems is the separation of knowledge about the problem from the data processing mechanisms. This is a fundamental difference compared to typical computational systems, where processing mechanisms are encoded in source code. Currently, advanced expert systems are increasingly used not only for comprehensive monitoring of equipment status on production lines [22] but also for controlling processes performed on these lines [23]. Among these solutions with significant application potential are programs based on FL methods. The method was originally introduced and developed as a tool for controlling processes where creating a model that precisely describes their behavior is difficult or impossible. This approach was firstly proposed by Zadeh, who published his work [24] and subsequently expanded on it in [25]. The FL introduced by this researcher is based on causal relationships and enables the effective processing of incomplete or imperfect information, with computations reflecting the mechanisms of human reasoning. Input variables are defined, which may include, for example, measurement results of process parameters, and output variables, which define system responses. The interactions between variables are described by rules in the form of causal dependencies, such as IF X_1 is A_1 and / or X_2 is A_2…THEN Y_1 is B_1 and / or …, where X_n represents a premise (simple or complex logical expression), and Y_n represents a conclusion (statement or decision). The fuzzy system is responsible for processing information entered into the system's knowledge base. Currently, fuzzy controllers are used as tools for controlling or monitoring the progression of deformation processes in near-real-time conditions, with interesting examples found in specialized publications. For example, in [26], the problem of selecting the most advantageous parameters for sheet metal stamping was addressed using three methods. These methods included an analysis based on displacement of points, a fast and approximate decision-making method using FL, and an approach combining the two previous methods. Manabe et al. [27] employed this method as a tool to determine the optimal loading path in the tube hydroforming process. Raßbach and Lehnert [28] utilized FL for analyzing the flow of gradient materials during their plastic deformation. Fuzzy models have been successfully used to predict material flow during processing [29]. Lee and Kopp [30] presented the concept of adapting an FL-controller for a hydraulic forging machine. In turn, Gronostajski et al. [31] developed an innovative expert system for analyzing the key mechanisms responsible for tool wear in selected hot forging processes on industrial lines. Lin et al. [32] developed a fuzzy expert system to estimate dimensional errors in forging products with complex shapes. Meanwhile, Wójcik et al. [33] used an algorithm based on the FL soft-computing method to assess parameters influencing the strengthening of S235JR construction steel under cyclic loading. The FL has also found applications in designing new deformation processes [34]. Implementing alternative production lines for hot deformation methods aims to improve process reliability or shorten the technological chain. However, operational and strategic decisions, especially those made at early stages of design, are often based on subjective criteria and introduce significant uncertainty regarding their outcomes. This often leads to incorrect solutions, resulting in costly modifications to tools or equipment. The causes of these issues include data gaps or uncertainty about their accuracy once implemented into new technologies. One method that offers a chance to avoid these problems is the parameterization of causal relationships and their fast analysis using FL-controllers.

It is well known that flow curves, supported by microstructural analysis, can be used as a basis for developing mathematical descriptions of the behavior of the material under deformation, in the form of appropriate models. Currently, it is commonly assumed that FL is applicable when data are incomplete or imprecise. On the other hand, if models describing the process are available, this method is considered unnecessary. However, it should be noted that the nature of changes in the actual stress values during hot deformation and the microstructure after deformation will depend on the complex interaction of a range of factors [29]. These factors include the initial microstructure, temperature and its changes during the process, the kinetics of work hardening and recrystallization phenomena, the strain value, strain rate, loading method, and others [35]. This information can be analyzed using fuzzy set theory. Such an approach allows for the development of an integrated system using FL that operates in near-real-time. The basis for analysis in this case would be the results of ongoing measurements of process parameters on the production line. Consequently, the fuzzy controller's operation could involve not only monitoring process parameters but also their fast analysis and adjustment. The goal should be to maintain favorable process conditions and achieve the desired microstructure of the products. This application of FL is the subject of broader research conducted by the authors, with one of the challenges being the development of a foundation for constructing an

FL-controller to control the multi-stage open die hot forging process of 80MnSi8-6 steel.

In the authors' opinion, supported by literature analysis and their own research findings, FL can be effectively used as a tool for fast estimation of advantageous parameters for hot deformation of various materials, based on data from experiments and their detailed analysis. An example of research conducted in this field includes the development by the co-authors of this publication of an FL-controller designed for the fast selection of optimal hot shaping parameters for titanium alloys [36]. The demonstrated application potential of such an approach also motivated the continuation of research in this area.

2 Experimental procedure

2.1 Purpose and scope of research

The aim of the research presented in this work was to develop a FL-controller for estimating the optimal parameters for hot deformation of 80MnSi8-6 steel, based on results from plastometric tests, analysis of their outcomes, observations of the microstructure of deformed samples, and calculations using DRX models and finite element method (FEM) numerical analysis, including microstructure evolution modeling. In the first phase, the research focused on analyzing the results of compression tests on 80MnSi8-6 steel, including the flow curve profiles and the positioning of characteristic points on these curves. It also involved observing the microstructure of deformed samples, determining the average austenite grain size, preparing a material information database as a basis for applying knowledge engineering, developing the FL-controller, and verifying the accuracy of the controller's calculations by comparing them with FEM numerical modeling results. The subsequent phase of the research involved designing an FL-controller for analyzing DRX kinetics based on data obtained from an original model of this phenomenon. The accuracy of the controller's performance was verified by comparing the estimated DRX volume fraction with the distributions of this value determined through both the model and FEM analysis.

2.2 Examined material

The material investigated was 80MnSi8-6 steel, obtained by casting process followed by preliminary hot forging of the ingot. The chemical composition of the steel is summarized in Table 1, and images of its microstructure in the as-delivered state are shown in Fig. 1. The microstructure of the starting material consists of several phases. Bright areas corresponding to ferrite grains can be distinguished, along with areas where pearlite grains are present, visible as alternating lamellae of ferrite and cementite. Bainite is observed as dark areas with a layered structure. Ferrite exhibits highly varied morphology, with both large grains, typically of irregular shape, and smaller grains with a more regular shape.

2.3 Methods of investigation

Metallographic investigations of the material were conducted using Leica DM4000M light microscope. Samples for microstructural observation were prepared following a standard metallographic procedure, which involved grinding, polishing, and then etching with a 5% solution of nitric acid in ethyl alcohol. Quantitative analysis of the prior austenite grain size was performed using Metilo® software, which is used for quantitative microstructural analysis. The procedure for revealing austenite grains included annealing the samples at 350 °C for 72 h, cooling the samples with the furnace, and then etching the primary austenite grain boundaries. The etching procedure was adjusted individually based on temperature and strain rate to achieve satisfactory results.

The plastometric tests were conducted using the WUMSI (Warmumformsimulator, BÄHR-Thermoanalyse GmbH). Cylindrical samples with a diameter of 10 mm and a height of 18 mm were used. The faces of the compression specimens were polished. Before testing, the surfaces were coated with a layer of a lubricant to reduce the coefficient of friction. were placed in a heat-resistant steel container, heated in a furnace to 1250 °C, and then cooled to the deformation temperature. In the next step, the samples were compressed

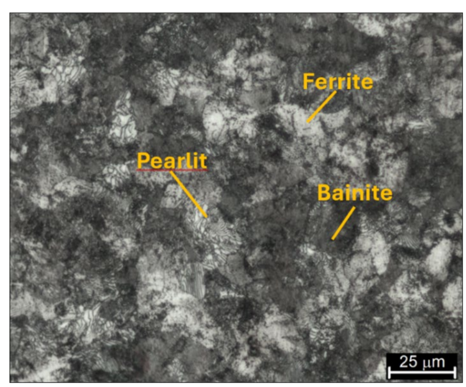

Fig. 1 Microstructure of 80MnSi8-6 steel in as-delivered state

Table 1 Chemical composition of 80MnSi8-6 steel [wt. %]

Chemical element	C	Si	Mn	P	S	Cr	Mo	V	Fe
Content, % by mass	0.79	1.55	1.9	0.003	0.003	1.3	0.25	0.11	Balance

at a constant strain rate. The compression tests were performed using strain rates of 0.1, 1.0, 10, and 20 s^{-1} at temperatures of 900, 1000, 1100, and 1250 °C, respectively, and were conducted until an true strain value of $\varepsilon = 1.2$ was achieved. After deformation, the samples were removed from the container and rapidly water-cooled. Detailed information on the procedures for conducting tests using the WUMSI simulator can be found in [18].

To accurately determine the true stress values during the hot compression tests, corrections accounting for the effects of friction and adiabatic heating were applied. In post-processing, the raw flow curves were corrected to eliminate the value of the stress that is necessary to overcome the friction forces. This value depends on the friction coefficient and the ratio between the height and diameter of the specimen at a given stage of the test. Calculations were performed step by step, for all successive stress values. Necessary corrections were incorporated, methods such as the Hensel-Spittel method and the Siebel equation were employed [37, 38]. Material data, including density, coefficient of friction, and thermal conductivity of the tested steel, were used to precisely determine the true flow stress during the correction process.

The FL computations were performed using the Fuzzy Logic Toolbox in Matlab. An approach based on Mamdani's criteria was employed. The defuzzification operation was carried out using the centroid method.

Numerical simulations of the hot compression test under isothermal conditions were conducted using FEM with the QForm UK v.10.2.1 software. The material was modeled as an isotropic, incompressible continuum. The software performed calculations based on a rigid-visco-plastic model with strengthening, where the flow stress is dependent on strain value, strain rate, and temperature. The range of elastic deformations was not analyzed. For the analysis of microstructural evolution, a modified Johnson–Mehl–Avrami–Kolmogorov (JMAK) model was employed [39]. The calculations accounted for heat generated during deformation. Friction was described using the first law of Levanov. Flow curves, developed from plastometric tests, and thermal characteristics of the material, determined for 80MnSi8-6 steel in the hot deformation temperature range, were input into the QForm UK software to describe the material's rheology.

3 Results

3.1 Plastometric tests as a foundation for building an FL-controller

Based on the data obtained from the hot compression tests on the WUMSI simulator for 80MnSi8-6 steel at the specified strain rates and temperatures, true stress–true strain curves were developed. The flow curves are presented in Fig. 2. The flow curves exhibit the typical sensitivity of bainitic steels to temperature and strain rate. Their behavior changes systematically with increasing temperature, which is observed across all strain rates used in the tests. At the lowest strain rate of 0.1 s^{-1} (Fig. 2a–d), the material exhibits flow at a nearly constant true stress value beyond a true strain of approximately 0.4. Equilibrium is reached in this range of true strain values regardless of the test temperature. For higher strain rates of 1 and 10 s^{-1}, there is a noticeable trend of a slight decrease in true stress with increasing true strain. At a strain rate of 20 s^{-1}, this trend becomes more pronounced, with the inflection point of the curve occurring at higher true strain values, around 0.5. A similar course of curves developed for the lowest tested temperature and in the strain rate range of 1—10 s^{-1} was observed (Fig. 2a). This demonstrates the low sensitivity of the tested steel to changes in strain rate under these conditions. This effect is particularly evident in values of true strain above 0.6, where the mechanisms responsible for the softening effect of the material dominate. In the initial stage of deformation, where mechanisms related to the generation and accumulation of dislocations at grain boundaries dominate, a change in strain rate has a slightly greater effect on the course of the curves. A more detailed analysis of the flow curves for 80MnSi8-6 steel is provided by Zyguła et al. [39], which aimed at developing models for microstructural evolution and the kinetics of the DRX phenomenon.

A quantitative and qualitative analysis of the flow curves for 80MnSi8-6 steel, aimed at preparing data for the construction of an FL-controller, was carried out according to the scheme shown in Fig. 3. Flow stages were developed for a representative flow curve of 80MnSi8-6 steel, derived from compression testing on the WUMSI simulator at a temperature of 1100 °C and a strain rate of 0.1 s^{-1} (Fig. 2c). In addition, the microstructure of the deformed sample was added on the schematic.

The schematic identified the various flow stages, mechanisms responsible for their occurrence, and key points necessary for the quantitative analysis of the phenomena occurring during hot deformation. The flow curve reveals three fundamental stages of deformation, which result from the activation or deactivation of specific mechanisms [40, 41]. In the initial stages of deformation, the flow stress increases significantly due to the formation and accumulation of structural network defects, mainly dislocations. During this stage of compression, WH and DRV are observed. This state persists until the critical strain (ε_c) is reached. Achieving this critical strain transitions the material into Stage II of flow. Since determining the ε_c from the stress–strain curves is challenging, a double-differentiation method [42] is commonly employed. Once the accurate value of the ε_c is

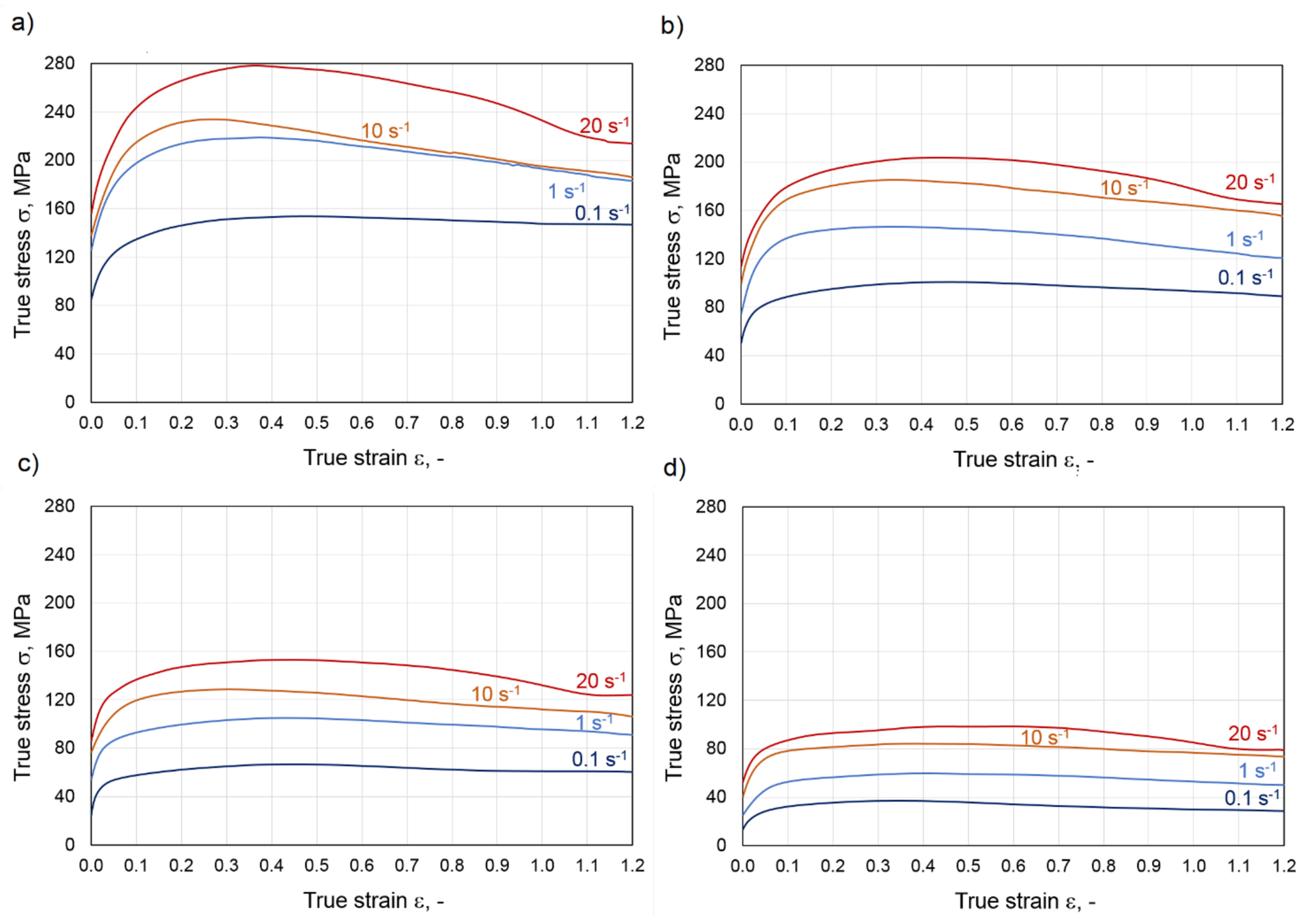

Fig. 2 Influence of thermo-mechanical parameters of hot compression tests using the WUMSI thermo—mechanical simulator on the courses of flow curves of 80MnSi8-6 steel developed on their basis. Temperature: **a** 900 °C, **b** 1000 °C, **c** 1100 °C and **d** 1250 °C

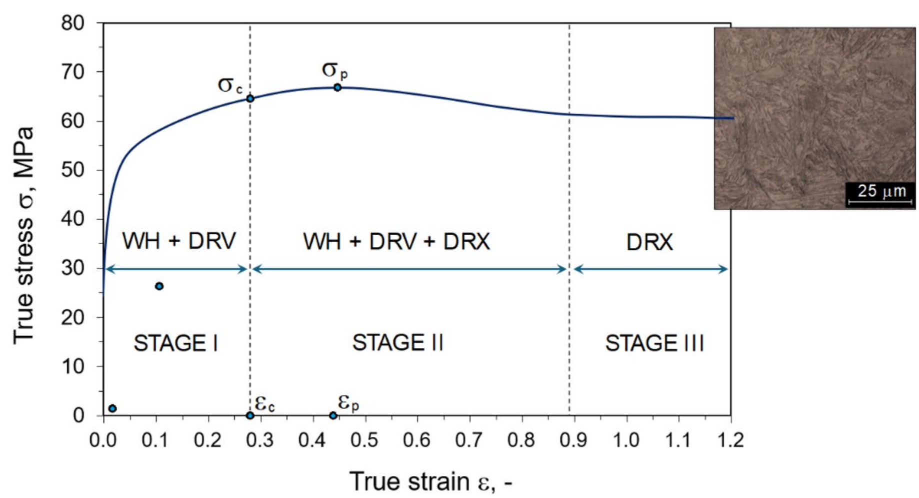

Fig. 3 Flow stages of 80MnSi8-6 steel during a hot compression test on a WUMSI simulator at 1100 ℃ and a strain rate of 0.1 s^{-1} (Fig. 2c), along with the microstructure of the deformed sample

established, DRX in the second sub-process can be derived from the experimental data of the first sub-process as well as the dislocation density theory [43]. As deformation continues, there is a gradual decrease in the rate of increase in true stress with further deformation because, at this stage, the DRX mechanism is activated, counteracting the effects of WH. Consequently, the true stress reaches a maximum value (σ_p) at what is known as the peak strain (ε_p). After this peak, as deformation progresses, the true stress gradually decreases. The final observed stage on the stress–strain curves is Stage III, known as steady-state flow. During this stage, the effects of WH and dynamic softening (DRV and/or DRX) reach equilibrium. As a result, the material exhibits stable flow, characterized by a constant flow stress as the true strain progresses. This stability arises because the effects of work hardening and deformation softening counterbalance each other. The nature of the curve's progression and the positions of characteristic points provide crucial information about the material's response to external loads, depending on the temperature and strain rate applied during testing. Consequently, these aspects are essential for analyzing the kinetics of DRX and for developing models of microstructural evolution.

By analyzing the obtained stress–strain curves and applying the above-described procedure, the values of σ_p and ε_p were determined, as well as σ_c and ε_c. The results of these calculations are presented in Fig. 4. This approach provided not only a qualitative but also a quantitative description of the flow curves. These data were used as the foundational information for the next step, which involved the development of the FL-controller.

3.2 Analysis of average prior austenite grain size after deformation on WUMSI simulator

Directly after the hot compression tests, the samples were rapidly cooled to preserve the prior austenite grain for quantitative analysis. The procedure for analyzing grain size

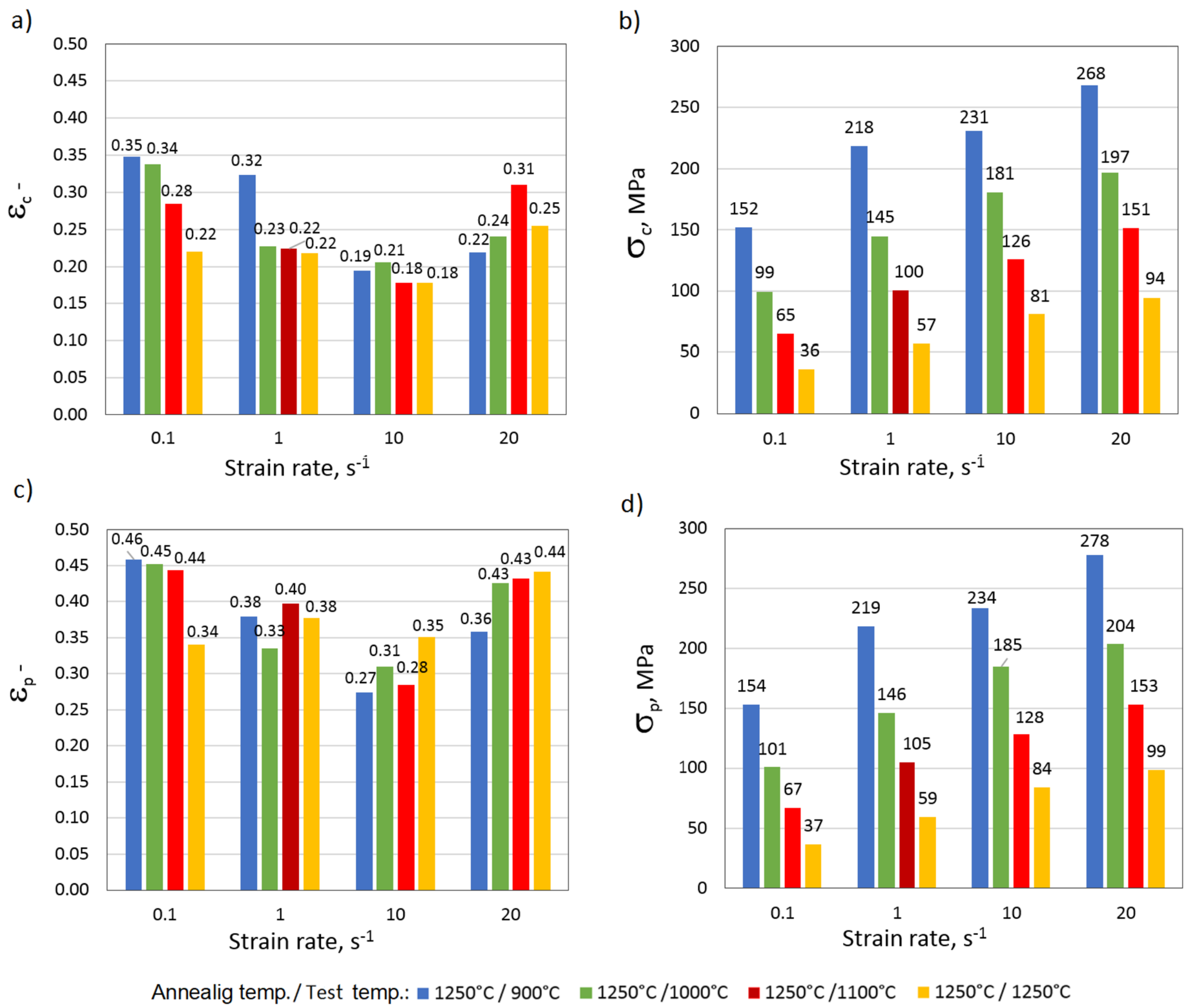

Fig. 4 The influence of compression test parameters on the WUMSI simulator on significant values of stresses and strains, determined on flow curves: **a** critical strain, **b** critical stress, **c** peak strain, **d** peak stress

using Metilo® software is illustrated in Fig. 5. The average initial grain size of 80MnSi8-6 steel was 526 µm. This value was determined for a sample that was heated to 1250 °C, held at this temperature for 240 s, and then rapidly cooled without deformation.

The results of the calculations for the prior austenite grain size of the samples after deformation are presented in Fig. 6. For the investigated 80MnSi8-6 steel, within the tested deformation parameters, a general trend of either a slight increase in primary austenite grain size or maintaining its size at the same level with increasing test temperature was observed (Fig. 6). An exception to this trend was found in samples deformed at a rate of 0.1 s^{-1}, where increasing the test temperature from 1000 to 1100 °C led to a decrease in the average primary austenite grain size. In samples deformed directly from the austenitization temperature of 1250 °C, without previous cooling, the largest average grain size was observed, regardless of the applied strain rate. Increasing the strain rate from 0.1 to 10 s^{-1} led to a slight decrease in the prior austenite grain size, while tests performed at the highest applied strain rate of 20 s^{-1} resulted in an increase in grain size.

3.3 Development of FL-controller based on plastometric tests and microstructure analysis.

The Fuzzy Logic Toolbox module, a component of Matlab, was used for fuzzy analysis. The block diagram of the FL-controller module and how they interact with each other is summarized in Fig. 7.

The input and output variables for the FL-controller were defined. The inference process was activated for two input variables and five output variables. The input variables were the parameters from the hot compression test (temperature and strain rate), presented in logarithmic notation. Since the hot compression process was conducted under strictly controlled conditions to achieve a constant strain value of

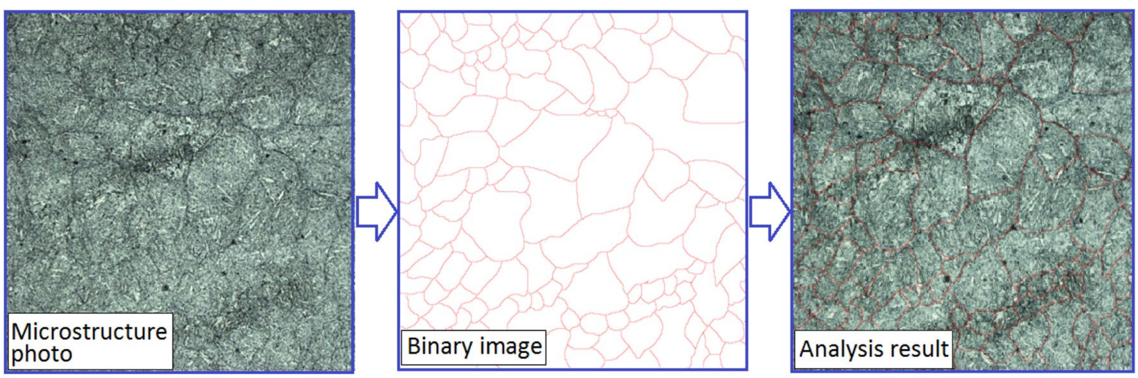

Fig. 5 Stages of analysis of prior austenite grain size in Metilo® software

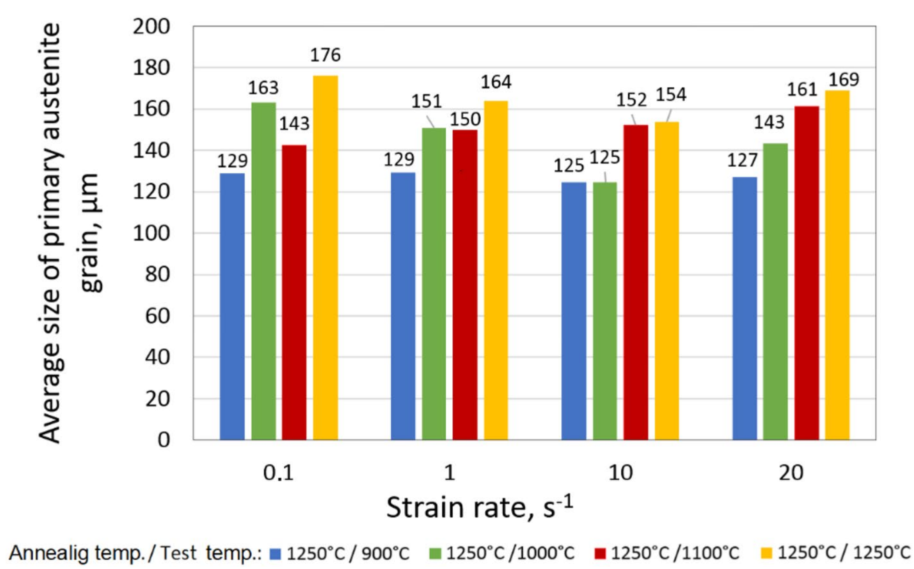

Fig. 6 The influence of compression test parameters on the WUMSI simulator on the average size of the prior austenite grain

1.2, other parameters and factors were assumed to be constant. The output variables chosen were those that allow for a quantitative description of the behavior of the studied steel during progressive deformation, applied under hot compression and at constant temperature and strain rate values. This behavior results from the progression of WH, DRV, and DRX phenomena. According to the schematic in Fig. 3, the kinetics of these phenomena can be defined by characteristic points on the flow curves, determined by values σ_p and ε_p, σ_c, and ε_c, respectively. The data was supplemented with information on the microstructure of the deformed samples, defined by the average prior austenite grain size, which varies depending on the compression test parameters. The procedure for determining the critical stress values is illustrated in Fig. 7 and Table 2. The first step involved defining the range of values for the input variables, temperature and strain rate (Fig. 8a). The characteristics of these values within the specified range were then represented using functions described with linguistic terms. For example, the variable "temperature" was described using the following terms and notations: "„minimal; MIN", "medium low; M_LOW", „medium big – MED_BIG and "maximal – MAX" (Table 2). The behavior of each function was represented as accurately as possible to reflect the dynamics of its changes within the analyzed range. This procedure was repeated for the input variable "strain rate" and for the output variables: "critical stress," "critical strain," "peak stress," "peak strain," and "average grain size," as illustrated in Fig. 8b. For the example output variable, "critical stress," the functions were described in linguistic terms (Table 2), using terms such "small", "relatively big – REL. BIG" etc. The remaining variables were named and described using functions in a similar manner. To enable data analysis and interpretation by the system, the relationships between the input and output variables were described using a set of fuzzy rules based on IF…THEN conditional statements. These rules introduce data into the system analogously to how a human expert analyzes experimental data and determines relationships between them. A simplified example of a rule might be: IF "temperature" is "minimum" and "strain rate" is "slow", "THEN" "critical stress" is "relatively big" and so on. In this way, a linguistic model was developed, which forms the basis for the operation of the FL-controller. The rule base was primarily developed based on experimental results, but also using expert knowledge. This includes information about the effects of various phenomena associated with deformation under specific conditions, such as WH or softening, on the material's flow behavior and the microstructure state of deformed samples. The defuzzification process was carried out using the centroid method.

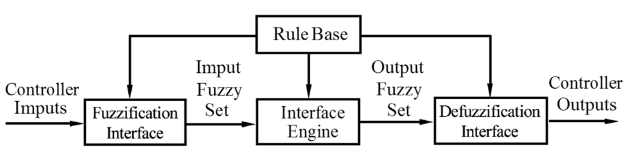

Fig. 7 Block diagram representing a FL-controller system

3.4 Results of FL analysis for selection of hot deformation parameters of 80MnSi8-6 steel

Figure 8 presents the dependencies calculated using the FL-controller between the test parameters of compression (temperature and strain rate), and their resulting changes in characteristic points on the flow curves (Fig. 8a–c) and the prior austenite grain size (Fig. 8d). These dependencies reflect the operation of the designed FL-controller. A comparison of these dependencies with the data obtained from the analysis of flow curve behavior and quantitative assessment of microstructure, as shown in Figs. 4 and 6, demonstrated a very good agreement. This indicates that the method used in the design and scaling of the controller to describe individual variables through functions and rules defining interactions between variables is correct. However, to verify the accuracy of this statement, precise validation of the controller's performance was required, which was conducted in the subsequent stage.

Table 2 A procedure for converting the values of the input variables; deformation temperature and strain rate and the output variable "critical stress" into their description using linguistic descriptions

Data from calculations					Linguistic description of the data				
WUMSI strain rate, s^{-1}	WUMSI test temperature, °C				Description of strain rate, s^{-1}	Description of WUMSI test temperature, °C			
	900	1000	1100	1250		MIN	M_LOW	MED_BIG	MAX
0.1	152.2	99.5	64.7	35.6	SLOW	REL. BIG	QUITE MEDIUM	REL. MEDIUM	SMALL
1.0	218.2	144.9	100.5	56.8	MEDIUM	BIG	MEDIUM	QUITE MEDIUM	SMALL
10	231.0	181.0	125.8	80.9	FAST	BIG	QUITE BIG	MEDIUM	REL. MEDIUM
20	268.2	196.9	151.3	94.3	V FAST	VERY BIG	QUITE BIG	REL BIG	QUITE MEDIUM

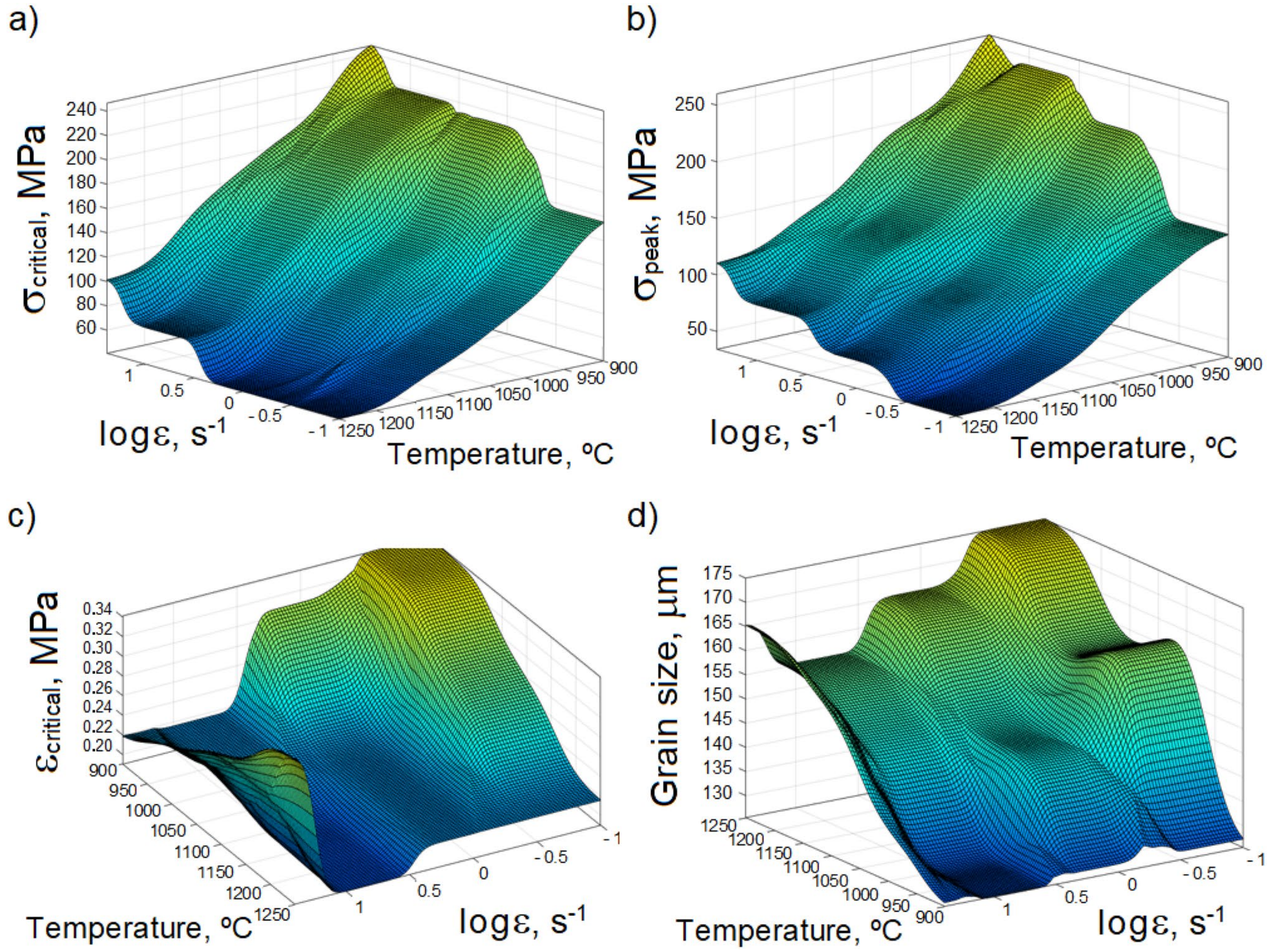

Fig. 8 Determined by the FL method, the relationships between temperature and strain rate during hot compression tests and the courses of change of the example output variables: **a** "critical stress", **b** "peak stress", **c** "critical strain", and **d** grain size"

3.5 Verification of the FL-controller

The accuracy of the FL-controller was verified. The purpose of this verification was both to confirm that the results of the calculations performed by the controller are correct and to demonstrate that the proposed approach based on knowledge engineering is appropriate and effective for the research problem analyzed. The verification process was conducted in two stages: quantitative and qualitative. In the first stage, the results of the controller's calculations were compared directly with the measurements and calculations derived from the flow curves and grain size data. In the second stage, a qualitative verification of the controller's performance was conducted. For this purpose, numerical simulations using FEM were developed and executed for selected variants of the compression process under constant temperature and strain rate conditions. The parameters and conditions for the hot compression process were set to be the same as those used during the tests on the WUMSI simulator. FEM modeling was conducted considering the evolution of microstructure, achieved by incorporating proprietary models developed for 80MnSi8-6 steel into the QForm UK software. The results obtained using the FL-controller were compared with the results of the FEM numerical modeling.

3.5.1 Comparison of FL-controller calculation results and experimental data

Figure 9 shows fragments of the Fuzzy Logic Toolbox module interface from Matlab, displaying the results of example calculations conducted using FL. The controller was provided with temperature and strain rate combinations that could be verified by comparing them with data obtained from experiments conducted under the same conditions. The set values of temperature and strain rate, recorded in logarithmic form, are indicated by vertical red lines. Table 3 presents the results of these calculations along with data obtained from the analysis of compression test results under the same conditions and measurements of the average prior austenite grain size. For both methods compared, very similar results were obtained, confirming the accuracy of the estimations made using the designed FL-controller.

3.5.2 Comparison of FL-controller calculation and FEM results

Numerical modeling that reflect the hot compression tests on the WUMSI simulator was conducted. Figure 10 shows the results of example simulations. The modeling results obtained at the final stage of the tests are presented, taking into account changes that occurred from the end of the test until the samples were quenched in water to maintain the original austenite grain. This period was estimated to be 4 s. The average grain size obtained from the FEM modeling was compared with measurement results and the calculations performed by the FL-controller (Table 3, Fig. 9). Figure 10a shows the results of a test conducted at 900 °C and a strain rate of 1 s^{-1}. The average grain size d_{av} in the center of the sample from FEM modeling was 127.5 μm. This value is very close to the measurement result d_{av} of the sample after deformation under these conditions on the simulator, which was 129.3 μm, and to the FL-controller calculation result of 127 μm. For FEM modeling of the average grain size at 1000 °C and a strain rate of 10 s^{-1} (Fig. 10b), the result was 123.7 μm, compared to 124.6 μm from the experiment and 127 μm from the FL-controller calculations. The average grain size from FEM modeling for hot compression at 1100 °C and a strain rate of 1 s^{-1} was 141.2 μm, with

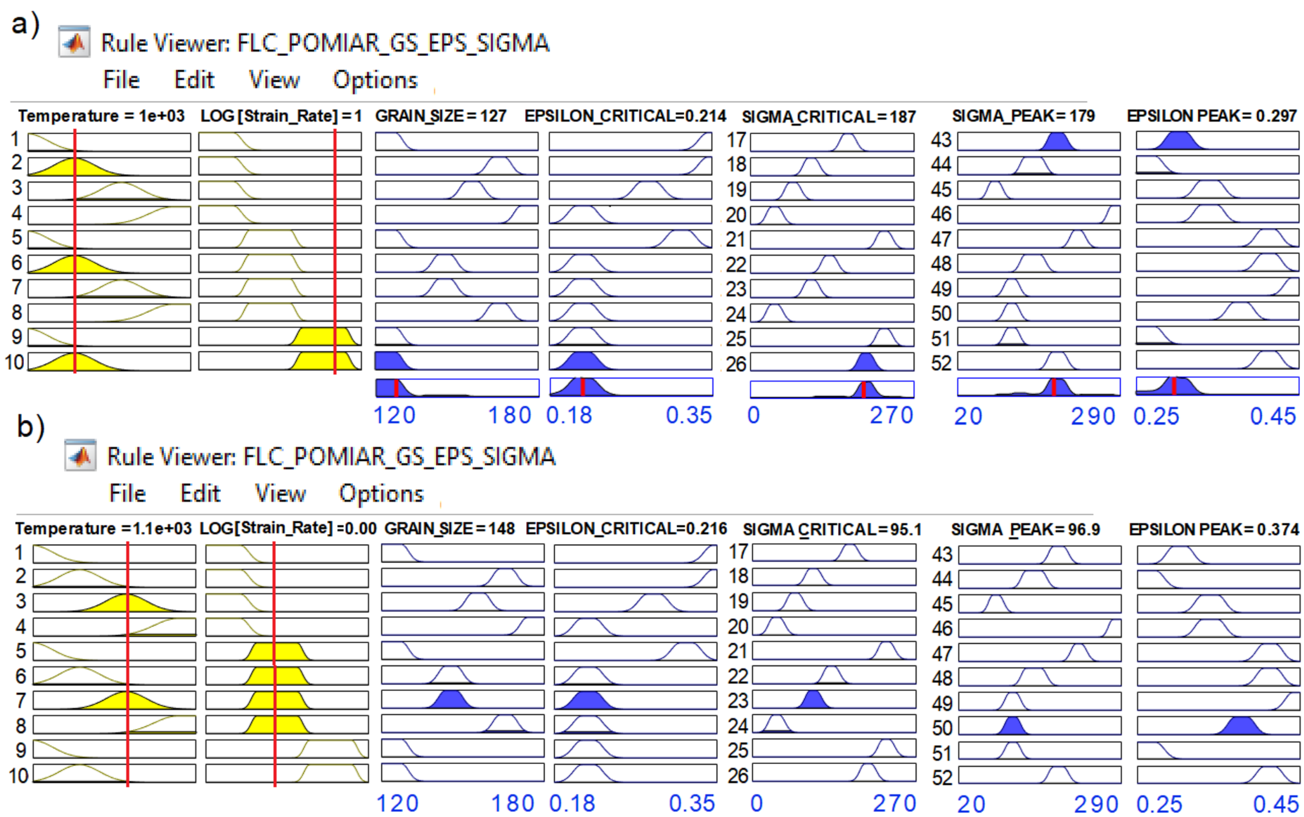

Fig. 9 Summary of selected results obtained by the FL method. Adopted deformation conditions: **a** temperature 1000 °C, strain rate 10 s^{-1}; **b** temperature 1100 °C, strain rate 1 s^{-1}

Table 3 Summary of calculations performed for selected variants of deformation temperature and strain rate by FL-controller in Fuzzy Logic Toolbox and experimental results

	T, °C	ε, s^{-1}	log $\dot{\varepsilon}$	Grain size, μm	ε_{c}, -	σ_c, MPa	ε_{p}, -	σ_p, MPa
FL calculations	1000	10	1	127	0.214	187	0.297	179
Experimental results				124.6 ± 7.4	0.205	181	0.310	185
FL calculations	1100	1	0	148	0.216	95.1	0.374	96.9
Experimental results				149.8 ± 16.7	0.224	100.5	0.397	104.7

The comparison was made for the test variants shown in Fig. 9

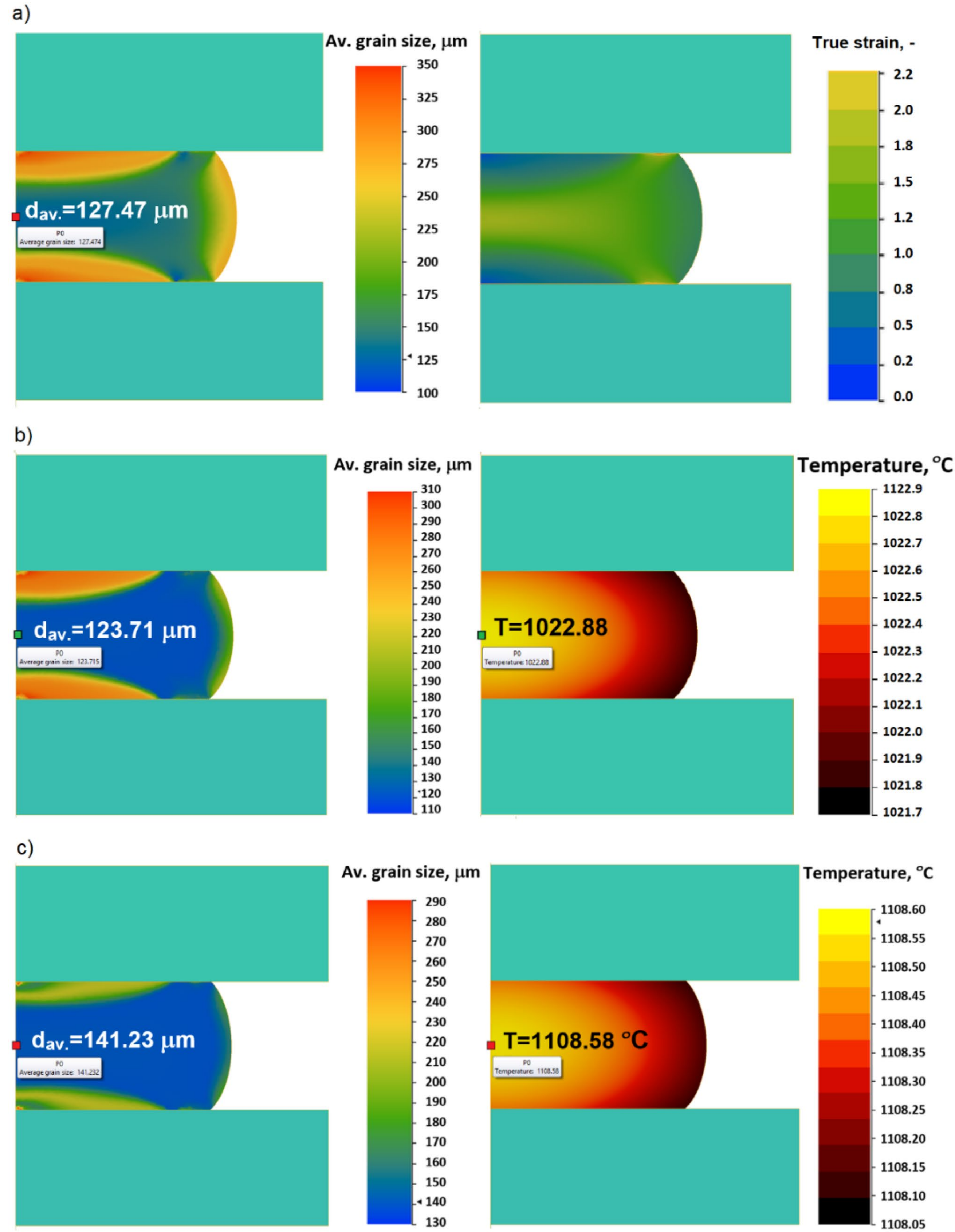

a)
Av. grain size, μm
350
325
300
275
250
225
200
175
150
125
100
dav.=127.47 μm
P0
Average grain size: 127.474
True strain, -
2.2
2.0
1.8
1.5
1.2
1.0
0.8
0.5
0.2
0.0
b)
Av. grain size, μm
310
300
290
280
270
260
250
240
230
220
210
200
190
180
170
160
150
140
130
120
110
dav.=123.71 μm
P0
Average grain size: 123.715
Temperature, °C
1122.9
1022.8
1022.7
1022.6
1022.5
1022.4
1022.3
1022.2
1022.1
1022.0
1021.9
1021.8
1021.7
T=1022.88
P0
Temperature: 1022.88
c)
Av. grain size, μm
290
280
270
260
250
240
230
220
210
200
190
180
170
160
150
140
130
dav.=141.23 μm
P0
Average grain size: 141.232
Temperature, °C
1108.60
1108.55
1108.50
1108.45
1108.40
1108.35
1108.30
1108.25
1108.20
1108.15
1108.10
1108.05
T=1108.58 °C
P0
Temperature: 1108.58

◂**Fig. 10** Summary of the results of FEM modeling of the hot compression tests. The final state of the simulation, taking into account the time required to remove the specimen from the container and cool it in water (4 s). Modeled deformation conditions: **a** temperature 900 ℃, strain rate 1 s^{-1}, **b** temperature 1000 ℃, strain rate 10 s^{-1}, **c** temperature 1100 ℃, strain rate 1^{-1}

corresponding values of 148 µm from measurements and 149.8 µm from FL-controller calculations. The FEM analysis showed a slight increase in temperature in the center of the sample compared to the assumed temperature, as visible in Fig. 10b and c. This effect also occurs during actual compression tests, particularly at higher strain rates, due to the conversion of plastic deformation work into heat [44]. In practice, the temperature of the sample is monitored during the process, and differences between the actual temperature and the test temperature are accounted for when developing flow curves, using appropriate correction procedures. In addition, Fig. 10c shows the distribution of true strain across the cross-section of the sample at the final stage of the test. This distribution depends on temperature and strain rate and is closely related to the distribution of the average prior austenite grain size.

3.6 Development of FL-controller based on DRX kinetics model

In the case of monitoring hot deformation processes, one of the key issues is understanding the kinetics of DRX. Since plastometric tests are conducted until a specific strain value is achieved, the analysis and evaluation of the microstructure are limited to that strain value. In hot forging processes, the strain value depends on factors such as the geometry of the initial material, the shape of the final product, and the complexity of the process. Analyzing the DRX behavior over a wide range of strain values requires developing a model of this phenomenon based on the material's flow curves. This issue was addressed by Zyguła et al. at [39], which resulted in the development of a model for the volume fraction of DRX for 80MnSi8-6 steel. The model was determined by fitting experimental data from plastometric tests to a modified JMAK model. The obtained coefficients were then implemented into the QForm UK software.

$$X_d = 1 - exp\left[\beta_d \cdot \left(\frac{\varepsilon - \varepsilon_c}{A_d \cdot d_0^{Md} \cdot \varepsilon^{Nd} \cdot \dot{\varepsilon}^{Ld} \cdot \exp\left(\frac{Q_d}{RT}\right) + C_d}\right)^{k_d}\right] \quad (1)$$

where: X_d—volume faction of the DRX, d_0—initial grain size (526 mm),—$\dot{\varepsilon}$strain rate, ε—true strain, ε_c—critical strain, T—temperature, Q_d—activation energy, R—universal gas constant and: β_d equals to ln(1-XDRX). Normally, the referenced X_d for calculations of the dynamic recrystallization kinetics is taken as 0.5 (i.e., 50% of softening), so that $\beta_d = 0.693$. The A_d, L_d, M_d and N_d are experimentally determined coefficients, which are responsible for adjusting the effects of strain rate, initial grain size and strain value on the proportion of recrystallized volume respectively, and C_d is a correction coefficient.

All the data necessary to perform the calculation of volume fraction of DRX (X_d) in the QForm software are summarized in the supplementary material attached to the [39].

3.6.1 Construction of FL-controller using the results of X_d model calculations

Using the model consistent with Eq. 1, a sufficient amount of data was obtained to precisely develop the FL-controller, including those values not covered by the experiment. The controller was designed using the Matlab Fuzzy Toolbox module, analogous to the data analysis based on plastometric tests and microstructure studies in the post-deformation state (Sect. 3.3). Input variables were set as temperature, strain value, and strain rate in logarithmic notation. The output variable was the volume fraction of DRX. The changes in these values within the given range were represented by functions described using linguistic terms. Figure 11 shows examples of the plots and descriptions for the input variable "Temperature" and the output variable "DRX Percent". Calculations were performed for strain values ranging from 0 to 1.2, with increments of 0.1, strain rates from 0.1 to 20 s^{-1}, and additional experimental data values of 0.5 and 5 s^{-1}. The temperature range covered the full extent of the tests: from 900 to 1250 ℃, with step changes of 25 ℃. For this variable, functions were described using linguistic terms such as "heating required," "quite big," "medium," "maximum," and others (Fig. 11). Both for temperature and all other variables, descriptions were provided using linguistic terms that could be easily combined into cause-and-effect relationships, such as IF—THEN. Hierarchical relationships between values were considered, using terms like "small," "medium," "average," "slow," "fast," and others. The ability to use a larger dataset compared to the range of results obtained from the experiments allowed for the inclusion of more functions describing the variables, thus increasing the precision of variable descriptions and enabling the formulation of more accurate rules describing cause-and-effect relationships between input and output data.

Figures 12 and 13 present the relationships between the parameters of the hot compression test, particularly temperature, true strain, and strain rate presented in logarithmic notation, and the corresponding values of the volume fraction of DRX.

The results of calculations performed using the FL method and the co-authored model developed by Zyguła

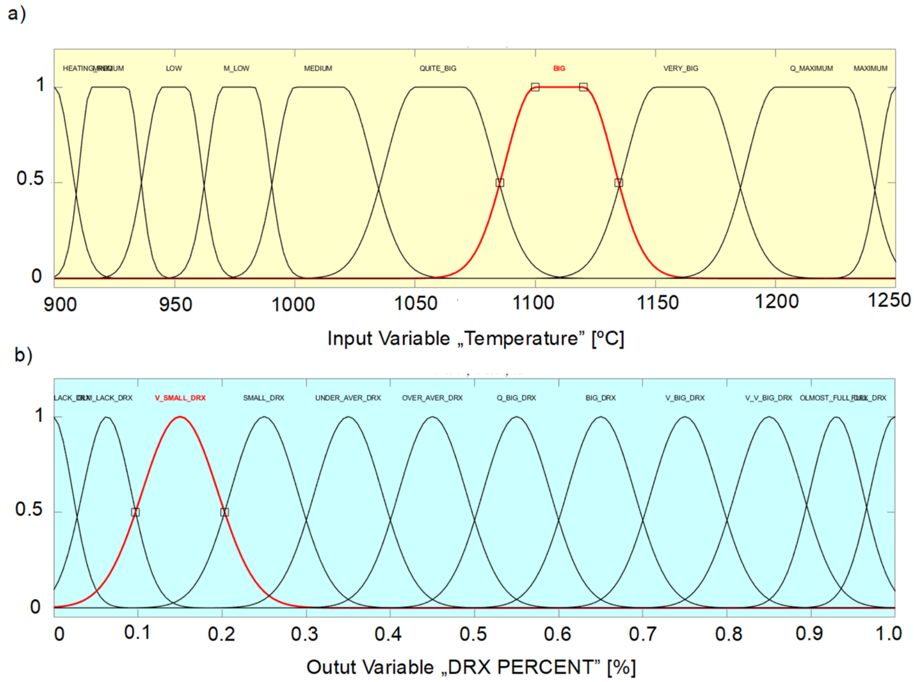

Fig. 11 Summary of courses and descriptions of: **a** sample input variable and **b** output variable

et al. [39] are compared. The relationships in Fig. 12a, c, e, and 13a, c reflect the operation of the designed fuzzy controller. The comparison between these relationships and the data obtained from calculations using the model (Figs. 12b, d, e, and 13b, d) show very good agreement. This confirms that the method of describing individual variables through functions, and the rules of interaction between variables introduced into the Fuzzy Logic Toolbox during the controller's design, were correctly designed and calibrated.

3.7 Comparison of volume faction of DRX calculations performed with FL-controller and FEM

Numerical modeling of the volume fraction of DRX during hot compression tests was conducted. The following boundary conditions were assumed during the FEM simulation: the friction coefficient based on Levanov's law was 0.4, which corresponds to the graphite lubricant used during the hot compression tests, the implemented material density varied from 7820 to 7730 kg/m3 in the temperature range of 40–1200 °C, the implemented thermal conductivity value was from 19.1869 to 26.7594 W/m·K in the temperature range of 600–1200 °C, and the specific heat was from 470 to 667 J/kg·K in the temperature range of 40–1200 °C. Figure 14 shows the results of FEM simulations carried out at a temperature of 950 ºC, which is critical for the occurrence of the DRX phenomenon. The calculations of X_d distributions in the QForm UK software were performed using Eq. 1, which is an integral part of the module used for microstructure evolution analysis. The calculations conducted with both the X_d model and the FL-controller (Figs. 12 and 13) confirmed that for a constant strain value of 1.2, a temperature of no less than 950 ºC is required for DRX to occur throughout the entire volume. Therefore, the calculations were performed for compression tests at this temperature, with strain rates ranging from 0.1 to 10 s^{-1}. Figure 14 shows the modeling results obtained at the final stage of the tests. The calculations took into account the time that elapsed from the end of the test until the samples were immersed in water to maintain the primary austenite grain. The FEM modeling results of the volume fraction of DRX distributions were compared with the results of calculations performed using the FL method. To this end, calculations using the FL-controller were also carried out for the modeled test variants, and their results are included in Fig. 14 (highlighted in green).

The value of X_d in the central region of the sample obtained through FEM modeling of the compression test at 950 ºC and a strain rate of 0.1 s^{-1} was 95.79%. This value is very close to the result calculated by the FL-controller, which estimated the X_d value under these conditions to be 97.8% (Fig. 14a). Increasing the strain rate to 1 s^{-1} (Fig. 14b) resulted in X_d values of 99.32% determined by FEM and 98.0% based on FL calculations. Applying a strain rate of 10 s^{-1} (Fig. 14c) led to X_d values of 99.4% from FEM and 97.9% from the FL method. However, regardless of the value of DRX (X_d) read at a representative point of the specimen, it should be noted that for a strain rate of 10 s^{-1}, the area on the cross-section where almost complete recrystallization occurs (Fig. 14c) is smaller than that determined by

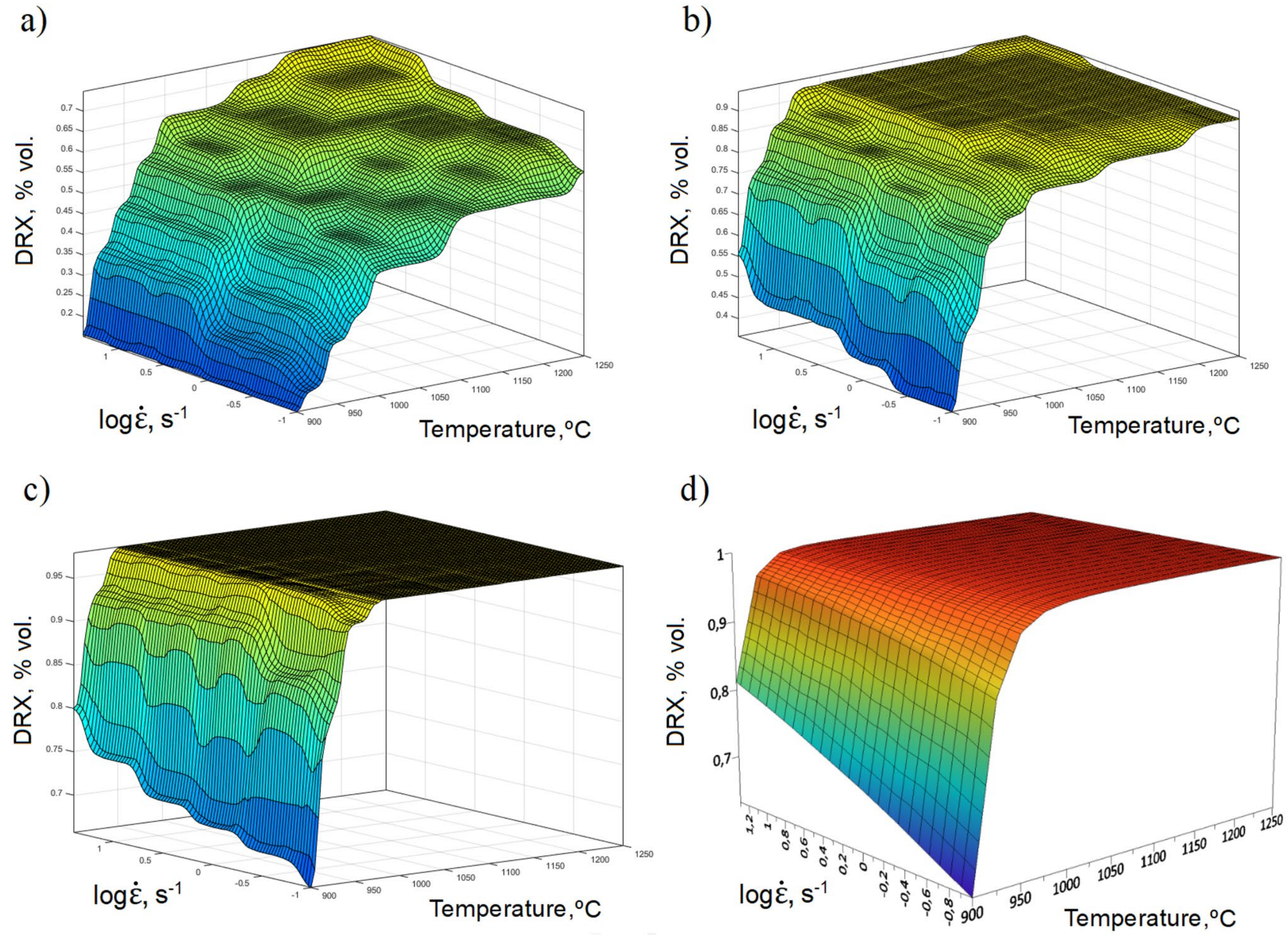

Fig. 12 Relationships of deformation parameters during hot compression tests and courses of change of volume faction of the DRX. Results of calculations; **a**-**c** by fuzzy logic method, and **d** by X_d model. True strain: **a** 0.8, **b** 1.0, and **c**,**d** 1.2

FEM for a specimen compressed at a strain rate of 1 s^{-1} (Fig. 14b), which is in tendency with the results obtained by the FL method. A comparison of the results obtained by both methods revealed differences of approximately 2%, regardless of the strain rate used. This comparison confirms that the FL-controller's estimations are highly consistent with FEM results, demonstrating the effectiveness and accuracy of the FL-based approach for predicting DRX behavior in various strain rate conditions.

4 Discussion

When designing hot forming processes, both qualitative and quantitative analysis of flow curves is essential for identifying fundamental phenomena associated with hot deformation, such as WH, DRV, and DRX. Another crucial part of information is the evolution of microstructure during deformation, particularly the average grain size of the primary austenite. Understanding these data and their interactions formed the basis for developing the FL-controller, which was built on the results of experimental research. The primary input variables for the controller were the basic parameters from the WUMSI simulator tests, such as temperature and strain rate in logarithmic notation. Since the hot compression tests were conducted under controlled conditions, other parameters and factors were assumed to be constant. The output variables chosen were those that allow a quantitative description the behavior of investigated steel during deformation under constant parameters. This behavior results from the progression of WH, DRV, and DRX phenomena, whose kinetics were analyzed through characteristic points on the flow curves, specifically σ_p, ε_p, σ_c, and ε_c. The final variable was the average grain size of the prior austenite, determined based on experimental studies. The procedure for converting the test parameters and their effects into variables described by linguistic terms, as detailed in subSect. 3.3, was carried out in a manner that enabled them to be analyzed by the FL-controller after defining an appropriate number of rules governing

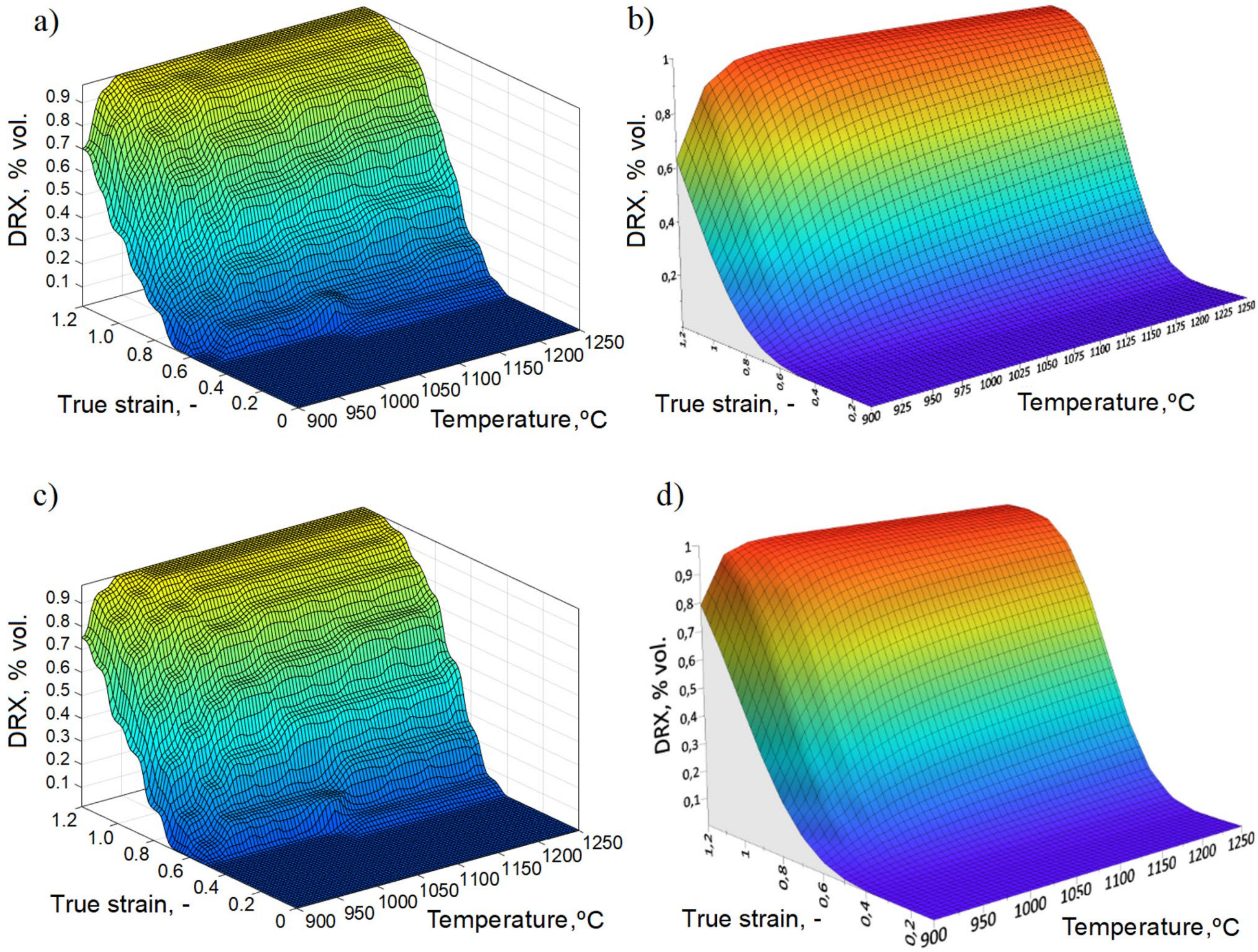

Fig. 13 Relationships of deformation parameters during hot compression tests and courses of change of volume faction of the DRX. Results of calculations; **a**-**c** by FL method, d-f by model. Calculations for log($\dot{\varepsilon}$): **a**,**b** 0.1, **c**,**d** 10. Results of calculations; **a**,**c** by FL method and **b**,**d** by X_d model

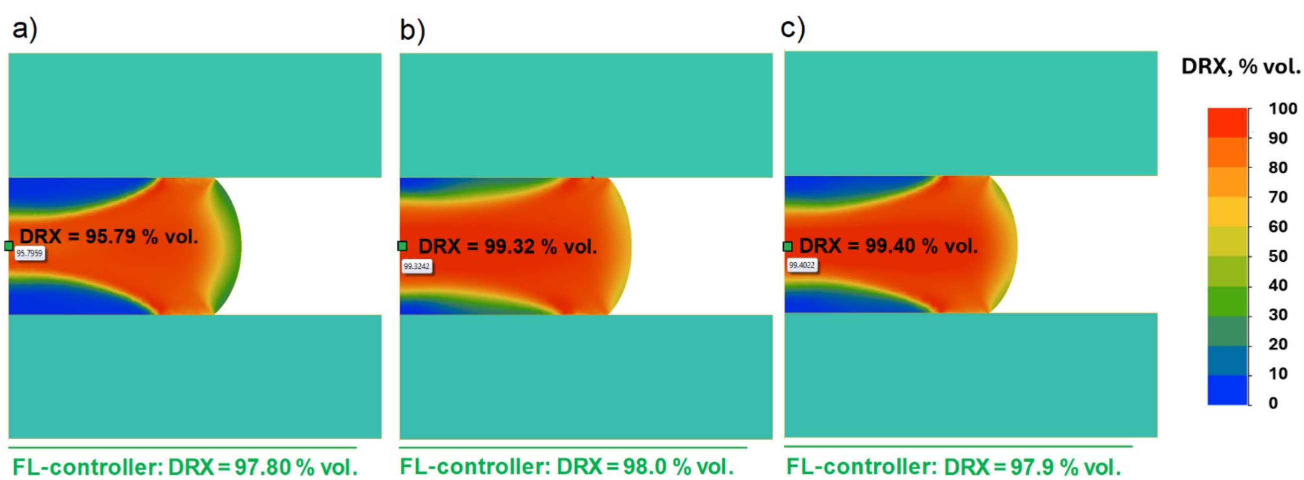

Fig. 14 Distributions of volume faction of DRX (X_d) on the cross-section of the deformed specimen obtained as a result of FEM modeling of hot compression tests and as a result of calculations obtained using FL-controller. Test temperature 950 °C, strain rate; **a** 0.1 s^{-1}, **b** 1 s^{-1}, **c** 10 s^{-1}

the process. When building an FL-controller, variables and functions can be described in any way. However, the closer the description of variables reflects how the human brain operates, the easier it becomes to formulate rules that accurately define the influence of interactions between the input variables on the output variables. The output data for analysis were derived from hot compression tests, particularly the flow curves and their characteristic points, as well as data on the microstructural state of deformed samples, such as the average prior austenite grain size. The analysis of these data is based on expert knowledge, where the expert identifies and interprets cause-and-effect relationships, recording them as IF–THEN rules. These rules define the operational strategy of the FL-controller.

Analyzing the relationships between temperature and strain rate versus the dimensions of the prior austenite grain size, as presented in Fig. 6, it can be concluded that the average grain size is influenced by specific combinations of these parameters. However, no clear trends in the impact of these parameters are observed across their entire range. The differences in grain size within the selected temperature and strain rate range are minimal, falling within a relatively narrow interval from 125 to 169 µm. The average grain size of 80MnSi8-6 steel, after being heated to 1250 °C, held at that temperature for 240 s (which was taken as the austenitization time in the WUMSI simulator test), and then cooled without deformation, was 526 µm. Comparing this value with the results of calculations for compressed samples leads to the conclusion that the hot deformation process of 80MnSi8-6 steel within the adopted thermomechanical parameters results in a significant reduction in the average austenite grain size. However, variations in the test parameters have a much smaller impact. This is an important observation, as it suggests the possibility of achieving a uniform grain size distribution during hot forming in industrial conditions, where the environment is non-isothermal and strain rates vary within the volume of the forging. Of course, this conclusion requires further verification.

When analyzing the relationships presented in Fig. 8 between temperature and strain rate during hot compression tests and the variations in output variables such as "critical stress," "peak stress," "critical strain," and "grain size," it is important to consider that the information input into the FL-controller, which determines its functionality, is not inherently part of its software. These inputs are derived from the selected variables, the way they are described through functions, and the interactions between these variables, as defined based on experimental results and their analysis. The program serves as a tool that formalizes these data and interactions into a form that can be processed by a system based on FL. Consequently, when these data are appropriately inputted, the calculation results produced by the controller can accurately reflect the experimental findings and the cause-and-effect relationships identified from them. Therefore, these results should be viewed as equivalent to a detailed data analysis performed by a human expert, but accomplished in a significantly shorter time. The result of this is the sensitivity to deviations in the results from regular value changes, as seen in Fig. 8, which are often "flattened" by models through averaging. This functionality of the FL-controller and its associated sensitivity allows for the consideration of deviations from trends in the response of a specific material to deformation under precisely defined conditions. Thus, the FL-based controller can identify effects that a human expert could detect. This distinction, in comparison to model-based programs, can often be an advantage of FL-controllers. Conversely, if necessary, an appropriate description of variables and the selection of rules can eliminate irregularities, thereby reducing the controller's sensitivity and basing its calculations on general trends.

To verify the functionality of the FL-controller, which was developed directly from experimental results, a comparison was made between the average prior austenite grain size in 80MnSi8-6 steel, determined using three different methods. Calculations were performed using the FL-controller in the Fuzzy Logic Toolbox, quantitative analysis on polished and etch cross-sections in the Metilo® software (Fig. 9, Table 3), and numerical simulation using the FEM method in QForm UK software, which accounted for microstructure evolution (Fig. 10). The results obtained were closely aligned, confirming that the FL-controller was properly designed and can be used for fast and accurate calculations of the average primary austenite grain size. It was also noted that in some parameter combinations, the FL-controller more accurately reflected the results obtained from measurements compared to the results from FEM numerical modeling. This conclusion is fully consistent with expectations, as the FL-controller was developed directly using data from compression tests and measurements of grain size after deformation. In contrast, models used for determining key values during plastic deformation are generally developed using widely accepted mathematical equations. The construction of such models involves analyzing data and fitting appropriate coefficients to the equations. These models are inherently designed to mathematically describe trends in the changes of the measured quantity and, as such, do not account for deviations from trends in individual measurements. Such deviations from standard relationships can be identified both by a human expert and by a well-developed FL system because the decision to include or exclude them in the calculations is within the competence of the person designing the controller. This approach offers an alternative to traditional models, as it can detect specific effects in the analyzed process or phenomenon that may indicate disturbances in typical behavior, which conventional models do not account for. If any deviation from the trend is classified as significant by the expert, it can be included in the calculations using the FL method, as the decision is up to the person designing or calibrating the FL-controller.

It is important to remember that the FL-controller operates on linguistic knowledge and performs operations on fuzzy sets. A key feature of this system is the separation of knowledge about the problem from the data processing mechanisms, which distinguishes it from other computational methods, such as those requiring the development and implementation of models. Numerical data are embedded within the ranges of variable values and the values of individual functions. However, the calculations are based on operations on fuzzy sets, in accordance with the rules introduced into the system. Therefore, only a precise selection of functions that describe the variables and the content of the rules will lead to results consistent with experimental outcomes, and this must be thoroughly verified. This operating mechanism is advantageous because a properly developed fuzzy controller is a flexible tool that can be relatively easily modified as needed. Adjustments to the controller, for example, in response to changes in process parameters or even the type of material, can be achieved by modifying the range of variables, altering the number and shape of functions describing individual variables, and by modifying, adding, or deactivating rules.

The developed, calibrated, and verified FL-controller, based on experimental data, allows for the fast estimation of the response of 80MnSi8-6 steel to changes in temperature and strain rate combinations within the accepted range. This enables the selection of optimal process parameters or the rejection of unfavorable variants. Input data for the controller can be provided not only manually but also through automatic real-time measurement of process parameters. In the latter case, the controller's response speed significantly increases, which is a major advantage of the method. Consequently, the controller can be used in industrial practice as a tool for the fast assessment of hot forging processes and the selection of advantageous process parameters. Real-time input of information on strain rate, which results from the dimensions of the charge and the speed of the machine's working parts, as well as the temperature of the charge, allows for the prediction of effects such as WH or softening, and estimation of the forces necessary for the process. Automation of the forging process implemented in a multistage system can provide a number of advantages, such as dimensional and shape precision, microstructure control, and stability and repeatability of the manufacturing [45]. Another advantage of the FL-controller is that the proposed solution does not require knowledge of mathematical models describing the process. At the same time, an approach based on human-like reasoning allows the detection of unusual effects that standard models may overlook. As noted by J.A. Stendal et al. [46], the deformation behaviour of alloys during hot deformation depends on a wide range of interrelated phenomena, such as WH, DRV, DRX or metadynamic recrystallisation (MRX) and heat generation. These phenomena can occur simultaneously and influence each other. It should also be considered that it is not only in hot forming processes that such phenomena occur but that rebuilding of the defective microstructure as a result of DRV can also occur in cold forming processes with large and very large deformation. The behaviour varies depending on the process temperature, the strain rate applied and the strain rate [47]. Therefore, a high-quality FL-controller based on the analysis of flow curves and microstructure can involve a large amount of information. In addition to rules describing obvious relationships (e.g., IF “temperature” is “very high” and “strain rate” is “very low” THEN “flow stress” is low), it is possible to incorporate into the analysis and reasoning those relationships that have a subtle nature and indicate, for example, the occurrence of recrystallization or process stabilization. Often, these rules describe trends typical for a specific alloy composition or for the method of preparing the charge for plastic deformation. According to the authors, this is one of the reasons why the proposed method is highly suitable for analyzing the behavior of materials during their hot deformation, including in the open die forging processes of 80MnSi8-6 steel.

In the subsequent stage, an innovative FL-controller was developed to analyze the kinetics of DRX occurring during hot deformation of 80MnSi8-6 steel, using data obtained from an original model of this phenomenon for its construction and calibration. It is commonly accepted that FL is applied in solutions where model development is impossible or too complex. The initial part of the work followed this model-free approach in constructing the FL-controller. However, in the next phase of the research, the authors applied a different approach, demonstrating the utility of FL methods even when a model is available, and highlighting the potential benefits of such a solution. Using an original model developed for the mathematical description of recrystallization kinetics, an adequate amount of data were prepared, describing the relationships between deformation parameters and the volume fraction of DRX. This dataset also included parameter combinations that were not covered by the experiments during hot compression tests. These data were used to develop and calibrate the FL-controller. Calibration involved adjusting the description of variables and modifying, adding, or deactivating rules describing interactions between variables. This procedure was continued until satisfactory agreement was achieved between the calculations performed by the FL-controller and those using the model. The results are graphically presented in Figs. 12c, d and 13. To verify the correctness of the FL-controller's operation, numerical modeling of the volume fraction of DRX for hot compression tests was carried out for an example temperature of 950 ºC and strain rates ranging from 0.1 to 10 s^{-1}. Comparison of the volume fraction of DRX distributions across the cross-section of the deformed sample obtained from FEM modeling of hot compression tests and the results calculated using the FL-controller (Fig. 14) demonstrated consistency between the results obtained by these methods. At the temperature of 950 ºC used for comparison, the differences in values were around 2%, regardless of the applied strain rate. This confirmed that the method of describing individual variables through functions and interaction rules defined in the form of rules was correctly designed. It should also be noted that using a strain value of 1.2 during the test leads to a non-uniform distribution of strain values across the cross-section of the cylindrical sample, due to the friction effect at the metal–tool interface, which is a known rule. This effect is illustrated in Fig. 10a. Consequently, the strain value in the central zone of the sample, where microstructure studies and grain size analysis are typically performed, differs from the average value. This effect influences the comparison results. Another factor affecting the FL-controller's performance is that operations on fuzzy sets require initial fuzzification of values at the beginning of the computational procedure and subsequent defuzzification to an averaged value at the final stage of calculations. Therefore, a 2% discrepancy between the FL-controller's estimates and the model calculations can be considered very good. This result strongly supports the assumption that the developed controller will accurately analyze microstructure changes caused by DRX under the hot deformation parameters that will occur on the production line. As a result, the FL-controller will function in place of the model, using real-time process parameter readings as input data. The argument for using an approach based on model-derived data for constructing the FL-controller primarily lies in the potential applications of such a solution. The authors have assumed that DRX analysis results obtained through the model can be directly used not only to assess the phenomenon’s behavior under controlled conditions, such as isothermal processes or those conducted at relatively high strain rates with minimal temperature drop. Their application could be significantly broader, as they may form a component in constructing FL-controllers for monitoring long-term processes, such as multi-stage free forging. In such processes, over time and with the decrease in the temperature of the material being shaped, phenomena like DRX, MRX, static recrystallization (SRX), and GG occur. The state of the microstructure at a given stage of the process results from the coexistence of these phenomena. The kinetics of these phenomena must be correlated with parameters such as temperature, time, strain rate, strain value, and the method of applying the strain. Due to the large number of variables involved, multi-stage processes are very challenging to control, and their modeling is complex. Possible solutions to this problem include FEM method that considers the complete evolution of the microstructure, the use of artificial intelligence, or methods based on knowledge engineering, including FL methods. The presently used computing packages based on FEM make it possible to determine many physical quantities which are difficult or impossible to experimentally [48]. This approach has been used, among others, by Hawryluk et al. [49]. However, FEM is time-consuming and, for this reason, allows for complex technological design, but is not suited for fast process control and real-time modifications. On the other hand, training neural networks requires a relatively large amount of data. The advantages of FL in this context are its flexibility, the smaller amount of data required to design the controller, and, if needed, the ability to respond to deviations from general trends that can be identified and interpreted by a human expert. Therefore, the designed FL-controller can be used in industrial practice, including for controlling multi-stage hot free forging processes of 80MnSi8-6 steel. An example of a complex hot forming of a product from 80MnSi8-6 steel, which, according to the authors, can be controlled using FL, is the technology of multi-stage forging presented in the work [18]. The process developed in this work consists of a series of operations occurring under conditions of changing temperature and deformation degree in the volume of the workpiece. It also requires the use of several sets of tools and the use of inter reheating operation. The designed FL-controller can be used to control those process steps during which the DRX mechanism is activated.

5 Conclusions

Research on the application of FL as a method for analyzing the hot deformation processes of 80MnSi8-6 steel, conducted using data obtained from flow curves, microstructure analysis, DRX phenomenon modeling and numerical analysis combined with microstructure evolution modeling, has led to the following conclusions:

1. A well-designed FL-controller allows for fast assessment of the response of hot deformed material to specific combinations of temperature and strain rate. It also enables predicting the impact of deformation parameters on the work hardening and softening behavior, as well as the microstructure, particularly the average prior austenite grain size.
2. Data obtained from experiments, such as the analysis of flow curves developed from plastometric tests or the assessment of the microstructure after deformation, can be used for developing and calibrating the FL-controller.

3. The development of an FL-controller based on DRX phenomenon modeling resulted in a precise tool that can be used for controlling short-term processes or those conducted under isothermal conditions. It can also be integrated into a complex FL-controller for managing stages of long-term processes where DRX occurs.
4. The proposed solutions are useful in industrial settings both when it is not possible to use models describing microstructure changes during hot deformation of 80MnSi8-6 steel and when the speed of the control system's response is a priority.
5. The FL-controller's response speed can be enhanced by automating real-time measurement of process parameters and directly inputting the results into the FL system. This method allows for obtaining expert analysis results, based on causal relationships and beyond typical computational procedures, in a significantly shorter time than a human expert. These results can then be automatically entered into the process control system.

Funding This study was funded by the National Science Centre, Poland under "M-ERA.NET 2 Call 2020", Grant No. 2020/02/Y/ST8/00107.

Data availability The data that support the findings of this study are available from the corresponding author upon reasonable request.

Declarations

Conflict of interest The authors have no competing interests to declare that are relevant to the content of this article.

Ethical approval This article does not contain any studies with human participants or animals performed by any of the authors.

References

1. Yu Y, Lan L, Ding F, Wang L. Mechanical properties of hot-rolled and cold-formed steels after exposure to elevated temperature: a review. Constr Build Mater. 2019;213(20):360–76.
2. Bhadeshia HKDH. Atomic mechanism of the bainite transformation. J Heat Treatm Mat formerly HTM Z Werkst Wärmebeh Fertigung. 2017;72(6):340–5.
3. Zhang FC, Wang TS, Zhang P, Zhang CL, Lv B, Zhang M, Zhang YZ. A novel method for the development of a low-temperature bainitic microstructure in the surface layer of low-carbon steel. Scr Mater. 2008;59:294–6.
4. Królicka A, Żak A, Kuziak R, Radwański K, Ambroziak A. Decomposition mechanisms of continuously cooled bainitic rail in the critical heat-affected zone of a flash-butt welded joints. Mater Sci-Pol. 2021;39(4):615–25. https://doi.org/10.2478/msp-2022-0002.
5. Zhu Z, Han J, Li H, Lu C. High temperature processed high Nb X80 steel with excellent heat-affected zone toughness. Mater Lett. 2016;163:171–4.
6. Królicka A, Janik A, Żak A, Radwański K. The qualitative–quantitative approach to microstructural characterization of nanostructured bainitic steels using electron microscopy methods. Mater Sci-Pol. 2021;39(2):188–99. https://doi.org/10.2478/msp-2021-0017.
7. Avishan B, Talebi P, Tekeli S, Yazdani S. Producing nanobainite on carburized surface of a low-carbon low-alloy steel. JMEPEG. 2023;32:211–20.
8. Garcia-Mateo C, Caballero FG, Sourmail T, Smanio V, de GarciaAndres C. Industrialised nanocrystalline bainitic steels. Design approach. Int J Mater Res (formerly Z Metallkd). 2014;105(8):725–34.
9. Caballero FG, Bhadeshia HKDH, Mawella KJA, Jones DG, Brown P. Design of novel high strength bainitic steels: part 2. Mater Sci Technol. 2001;17:517–22.
10. Sourmail T, Garcia-Mateo C, Caballero FG, Morales-Rivas L, Rementeria R, Kuntz M. Tensile ductility of nanostructured bainitic steels: influence of retained austenite stability. Metals. 2017;7:31–7.
11. Marcisz J, Burian W, Rozmus R, Janiszewski J. Microstructural changes of the nanostructured bainitic steel induced by quasi-static and dynamic deformation. Arch Metall Mater. 2017;62(4):2317–29.
12. Sourmail T, Caballero FG, Garcia-Mateo C, Smanio V, Ziegler C, Kuntz M, Elvira R, Leiro A, Vuorinen E, Teeri T. Evaluation of potential of high Si high C steel nanostructured bainite for wear and fatigue applications. Mater Sci Technol. 2013;29(10):1166–73.
13. Leiro A, Vuorinen E, Sundin KGB, Prakash B, Sourmail T, Smanio V, Caballero FG, Garcia-Mateo C, Elvira R. Wear of nano-structured carbide-free bainitic steels under dry rolling-sliding conditions. Wear. 2013;298:42–7.
14. Du Y, Wang X, Zhang D, Wang X, Ju C, Jiang B. A Superior strength and sliding wear resistance combination of ductile iron with nanobainitic matrix. J Mater Res Technol. 2021;11:1175–83.
15. Sukumar G, Senthil PP, Reddy PRS, Singh BB, Ramakrishna B, Kumar KS, Madhu V. Ballistic efficacy of carbide free high strength nano-structured bainitic armour steels. Def Sci J. 2023;73(2):131–9.
16. Garcia-Mateo C, Caballero FG, Sourmail T, Cornide J, Smanio V, Elvira R. Composition design of nanocrystalline bainitic steels by diffusionless solid reaction. Met Mater Int. 2014;20(3):405–15.
17. Sourmai T. Bainite and superbainite in long products and forged applications. HTM (J Heat Treat Mater). 2017;72(6):371–8.
18. Wojtaszek M, Lisiecki Ł, Łukaszek-Sołek A, Korpała G, Zyguła K, Śleboda T, Jabłońska MB, Prahl U. Application of processing maps and numerical modelling for identification of parameters and limitations of hot forging process of 80MnSi8–6 steel. Arch Civ Mech Eng. 2023;23(4):240.
19. Duan XW, Liu JJ, Li P, Liu JS. Experimental study and numerical simulation of dynamic recrystallization behavior of a high-strength steel. Met Mater Int. 2021;27:1044–59.
20. Zhong T, Rao KP, Prasad YVRK, Gupta M. Processing maps, microstructure evolution and deformation mechanisms of extruded

AZ31-DMD during hot uniaxial compression. Mater Sci Eng A. 2013;559:773–81.
21. Zyguła K, Lypchanskyi O, Łukaszek-Sołek A, Korpała G, Stanik R, Kubiś M, Przybyszewski B, Wojtaszek M, Gude M, Prahl U. A comprehensive study on hot deformation behavior of the metastable β titanium alloy prepared by blended elemental powder metallurgy approach. Metall Mater Trans A. 2024;55:933–54.
22. Mazzoleni M, Sarda K, Acernese A, Russo L, Manfredi L, Glielmo L, Del Vecchio C. A fuzzy logic-based approach for fault diagnosis and condition monitoring of industry 4.0 manufacturing processes. Eng Appl Artif Intell. 2022;115:105317.
23. Norwisz J, Boryczko B, Hołda A, Kolenda Z. Thermoecological cost analysis of shaft and flash smelting processes of copper production—general approach. Arch Metall Mater. 2009;54(1):153–9.
24. Zadeh LA. Fuzzy sets. Inform Control. 1965;8:338–53.
25. Zadeh LA. Fuzzy algorithm. Inform Control. 1968;12:94–102.
26. Shafaie M, Biglari FR, Keneshlou M, Gharib AR. Blank shape optimization in sheet metal processing using a hybrid fuzzy-sensitivity method. Int J Comput Integr Manuf. 2023;36(4):511–23.
27. Manabe K, Suetake M, Koyama H, Yang M. Hydroforming process optimization of aluminum alloy tube using intelligent control technique. Int J Mach Tools Manuf. 2006;46(11):1207–11.
28. Raßbach S, Lehnert W. Modelling of the deformation behaviour of FGM by fuzzy logic. Comput Mater Sci. 1999;16:167–75.
29. Hassan MA, Yamaguchi K, Takakura N: A fuzzy model for prediction of material flow-stress in metal forming. 7th International conference on numerical methods in industrial forming processes (NUMIFORM 2001). Proceedings Paper: Simulation of Materials Processing: Theory, Methods and Applications, 2001, pp. 033–308.
30. Lee YH, Kopp R. Application of fuzzy control for a hydraulic forging machine. Fuzzy Sets Syst. 2001;118(1):99–108.
31. Gronostajski Z, Hawryluk M, Kaszuba M, Marciniak M, Niechajowicz A, Polak S, Zwierzchowski M, Adrian A, Mrzygłód B, Durak J. The expert system supporting the assessment of the durability of forging tools. Int J Adv Manuf Technol. 2016;82:1973–91.
32. Yin JL, Li DY, Peng YH. Knowledge acquisition from metal forming simulation. Int J Adv Manuf Technol. 2006;29(3–4):279–86.
33. Wójcik M, Gontarz A, Skrzat A, Winiarski G. Computational Methods of the identification of chaboche isotropic-kinematic hardening model parameters derived from the cyclic loading tests. ASTRJ. 2024;18(1):61–75. https://doi.org/10.12913/22998624/1759.
34. Weckenmann A, Akkasoglu G. Maturity determination of new forming processes considering uncertain indicator values. Key Eng Mater. 2012;502:97–102.
35. Stendal JA, Bambach M, Eisentraut M, Sizova I, Weiß S. Applying machine learning to the phenomenological flow stress modeling of TNM-B1. Metals. 2019;9:220.
36. Wojtaszek M, Zyguła K. Fast estimation of favorable parameters of hot metal forming, using the fuzzy logic method. Arch Metall Mater. 2023;68(2):723–31.
37. Christiansen P, Martins PAF, Bay N. Friction compensation in the upsetting of cylindrical test specimens. Exp Mech. 2016;56:1271–9. https://doi.org/10.1007/s11340-016-0164-z.
38. Sun CY, Qin Y, Liu Y, Xiao GQ, Zhang JS, Zhou J. Research on the hot deformation process of A100 steel based on high-temperature rheological behavior and microstructure. Materials. 2024;17(991):1–16. https://doi.org/10.3390/ma17050991.
39. Zyguła K, Cichocki K, Kowalczyk K, Puławski M, Korpała G, Wojtaszek M, Jabłońska M, Prahl U. Microstructure prediction of 80MnSi8-6 Steel after hot deformation based on dynamic recrystallization kinetics and FEM simulation. JOM. 2024;76:5193–209. https://doi.org/10.1007/s11837-024-06648-6.
40. Wang L, Liu F, Zuo Q, Chen CF. Prediction of flow stress for N08028 alloy under hot working conditions. Mater Des. 2013;47:737–45.
41. Chen M-S, Lin YC, Mac X-S. The kinetics of dynamic recrystallization of 42CrMo steel. Mater Sci Eng A. 2012;556:260–6.
42. Poliak EI, Jonas JJ. A one-parameter approach to determining the critical conditions for the initiation of dynamic recrystallization. Acta Mater. 1996;44:127–36.
43. Estrin Y, Mecking H. A unified phenomenological description of work hardening and creep based on one-parameter models. Acta Metall. 1984;32:57–70.
44. Jabłońska MB. Effect of the conversion of the plastic deformation work to heat on the behaviour of TWIP steels: a review. Arch Civ Mech Eng. 2023. https://doi.org/10.1007/s43452-023-00656-0.
45. Hawryluk M, Dudkiewicz Ł, Polak S, Barełkowski A, Mizejewski A, Szymańska T. Improvement of the technology of precision forging of connecting rod-type forgings in a multiple system, in the aspect of the possibilities of process robotization by means of numerical modeling. Materials. 2024;17(1087):2–18. https://doi.org/10.3390/ma17051087.
46. Stendal JA, Bambach M, Eisentraut M, Sizova I, Weiß S. Applying machine learning to the phenomenological flow stress modeling of TNM-B1. Metals. 2019;9(220):2–18.
47. Jabłońska MB, Kowalczyk K, Tkocz M, Chulist R, Rodak K, Bednarczyk I, Cichanski A. The effect of severe plastic deformation on the IF steel properties, evolution of structure and crystallographic texture after dual rolls equal channel extrusion deformation. Arch Civ Mech Eng. 2021;21(4):1–10.
48. Hawryluk M, Polak S, Rychlik M, Barełkowski A, Jakuć J, Marzec M. Development and implementation of die forging technology eliminating flange welding operations in conveyor driver forging. Materials. 2024;17(3281):1–18.
49. Hawryluk M, Rychlik M, Polak S, Zwierzchowski M, Dudkiewicz Ł, Marzec J, Jabłoński P. Analysis and improvement of an industrial process of hot die forging of an elongated forging tipped with a joggle with the use of numerical simulation results. ASTRJ. 2023;17(2):192–205.